

Article

# Composition and Morphology Characteristics of Magnetic Fractions of Coal Fly Ash Wastes Processed in High-Temperature Exposure in Thermal Power Plants

Dinh-Hieu Vu <sup>1,\*</sup>, Hoang-Bac Bui <sup>2,3</sup> , Bahareh Kalantar <sup>4</sup> , Xuan-Nam Bui <sup>1,5</sup>,  
Dinh-An Nguyen <sup>1</sup>, Qui-Thao Le <sup>1</sup>, Ngoc-Hoan Do <sup>1,6</sup> and Hoang Nguyen <sup>7,\*</sup> 

<sup>1</sup> Department of Surface Mining, Mining Faculty, Hanoi University of Mining and Geology, 18 Vien Street, Duc Thang Ward, Bac Tu Liem District, Hanoi 10000, Vietnam; buixuannam@humg.edu.vn (X.-N.B.); nguyendinhhan@humg.edu.vn (D.-A.N.); lequithao@humg.edu.vn (Q.-T.L.); dongochuan@humg.edu.vn (N.-H.D.)

<sup>2</sup> Faculty of Geosciences and Geoenvironment, Hanoi University of Mining and Geology, Hanoi 10000, Vietnam; buihoangbac@humg.edu.vn

<sup>3</sup> Center for Excellence in Analysis and Experiment, Hanoi University of Mining and Geology, Hanoi 10000, Vietnam

<sup>4</sup> RIKEN Center for Advanced Intelligence Project, Goal-Oriented Technology Research Group, Disaster Resilience Science Team, Tokyo 103-0027, Japan; Bahareh.kalantar@riken.jp

<sup>5</sup> Center for Mining, Electro-Mechanical Research, Hanoi University of Mining and Geology, 18 Vien Street, Duc Thang Ward, Bac Tu Liem District, Hanoi 10000, Vietnam

<sup>6</sup> Faculty of Mining, Saint-Petersburg Mining University, Saint-Petersburg 199106, Russia

<sup>7</sup> Institute of Research and Development, Duy Tan University, Da Nang 550000, Vietnam

\* Correspondence: vudinhieu@humg.edu.vn (D.-H.V.); nguyenhoang23@duytan.edu.vn (H.N.)

Received: 19 March 2019; Accepted: 16 April 2019; Published: 13 May 2019



**Abstract:** Coal-fired power stations are one of the primary sources of power generation in the world. This will produce considerable amounts of fly ash from these power stations each year. To highlight the potential environmental hazards of these materials, this study is carried out to evaluate the characterization of fly ashes produced in thermal power plants in northern Vietnam. Fly ash was firstly fractionated according to size, and the fractions were characterized. Then, each of these fractions was analyzed with regard to their mineralogical features, morphological and physicochemical properties. The analytical results indicate a striking difference in terms of the characteristics of particles. It was found that magnetic fractions are composed of magnetite hematite and, to a lower rate, mullite, and quartz. Chemical analyses indicate that the non-magnetic components mainly consist of quartz and mullite as their primary mineral phases. As the main conclusion of this research, it is found that the magnetic and non-magnetic components differ in terms of shape, carbon content and mineralogical composition. In addition, it was found that magnetic components can be characterized as more spheroidal components compared to non-magnetic ones. This comprehensive characterization not only offers a certain guideline regarding the uses of different ash fractions but it will also provide valuable information on this common combustion process.

**Keywords:** magnetic fraction; chemical properties; fly ash coal wastes; XRD analysis; thermal power plants

## 1. Introduction

Vietnam is the Southeast Asian country with the highest reliance on coal for electricity generation. Furthermore, with the rapidly increasing demand for electricity in Vietnam, recently the number of coal power plants have been expanded or been constructed. Presently, these coal-fired thermal power plants generate approximately 20% of the total electricity demand in Vietnam. As Vietnamese thermal power plants use domestically mined coal, this increase in coal-fired generation will lead to an increase in coal production within the country by companies such as Vinacomin (Vietnam National Coal and Mineral Industries Group). The stations sampled at for this study, Uong Bi and Pha Lai thermal power stations, procure coal from Vinacomin and have a capacity of approximately 1800 MW of electricity. To satisfy the increasing demands for electric power, the coal power plants are vital, but they also emit a large amount of fly ash and are among the causes of environmental problems, especially, the pollution related to coal fly ash. Currently, coal fly ash is used for various purposes: brick-making, landfilling, construction, soil amendment, and others [1–4]. However, effective end uses are possible only if a comprehensive characterization of fly ash produced at the plant can be carried out [5,6]. Also, a comprehensive characterization is expected to give useful information on the combustion processes.

Fly ash is a complex heterogeneous form of coal combustion residue. Fly ash is generally regarded as the finest particles that are formed (0.2–90  $\mu\text{m}$ ) because of the transformation of mineral matter (i.e., existing in coal particles) during combustion processes [7,8]. However, fly ash contains noticeable amounts of large (e.g., 90–300  $\mu\text{m}$ ) char, semi-cooked or coked carbon matters because of low combustion efficiency in combustors. The main weakness is because of low-quality control in maintaining the particle size of the pulverized coal feed, perhaps more than other factors. Besides, fly ash is characterized by irregular shape and contains vesicular, lacy, solid/hollow Alumino-siliceous spheres as well as an alumino-siliceous matter of complex elements [9].

Based on combustion conditions, the type of coal used, and removal proficiency of devices that control air pollution, the chemical composition of fly ash is variant [10]. As an example, in South African coal fly ash, the combined content of  $\text{Fe}_2\text{O}_3$ ,  $\text{Al}_2\text{O}_3$ , and  $\text{SiO}_2$  in fly ash must be over 70% whereas the CaO content should not exceed 5%. Therefore, the 2-step treated fly ash was added together that contains less than 50% of  $\text{Fe}_2\text{O}_3$ ,  $\text{Al}_2\text{O}_3$ , and  $\text{SiO}_2$  [11]. In this fly ash category, the CaO content changes in the range of 20 to 30%. However, the formulation of fly ash may differ to some extent by whether the same is true of fly ashes with low/high calcium or low/high iron [12]. As a result, they require different utilization schemes. Fly ash's mineralogical composition mainly depends on the geological features that inform coal formation and deposition, as well as the combustion condition [13–15]. Here, quartz [14,16–19], mullite [14,20–22], hematite [19,23–25], magnetite, and lime are the most common and predominant phases apart from other minor constituents [22,25–28]. Also, fly ash's mineralogical composition is determined by the type of coal used. So, anorthite, quartz, hematite, gehlenite, and mullite predominantly constitute the main crystalline phases in lignite fly ash [22,26,29–31]. In fact, quartz and mullite are the primary crystalline phases in low calcium fly ashes while high calcium fly ashes contain quartzite, C4AS, and C3A. The predominant minerals in fly ashes are mullite, quartz, hematite, magnetite, calcite, and dolomite.

As an important aspect of fly ash, morphology requires a thorough evaluation. It is well established that the particles of fly ash can be categorized in to eleven morphological groups based on the examination by light microscopy [10,14,20,32]. 'Char' is the most critical carbonaceous particle in fly ash that is formed when the coal particles are devolatilized. Resultant burning of char as well as transformation of intrinsic mineral matter conducts to generating ash particles (e.g., in the form of solid, irregular and hollow spherical particles) among which the most significant and value-added are cenospheres, planispheres and ferrospheres [33–37]. As the main objective of this study, we aimed to evaluate the fly ash produced in Uong Bi and Pha Lai thermal power stations. This study particularly revolves around the physical, morphological and chemical characterizations of the particles of the fly ash focusing on the size extent of the particles.

## 2. Materials and Methods

### 2.1. Sampling and Size Analysis

The fly ash samples were taken from two thermal power plants Uong Bi and Pha Lai power plants (sample UB and sample PL, respectively) in northern Vietnam. The Uong Bi and the Pha Lai power plants use pulverized coal combustion (PCC) technology and circulating fluidized bed combustions (CFBC) technology, respectively, for power generation. The samples were completely mixed after applying the coning and quartering method then wet sieved down to prepare a granular material smaller than  $<25\ \mu\text{m}$  in size. A hand-held permanent bar magnet was used to separate the magnetic particles from each size fraction.

### 2.2. Characterization

Particle characterization was performed for all the fractions by considering a variety of specifications and methods: density and size of particle, the weight percentage distribution, LOI (according to ASTM C311-04), mineralogical analysis (XRD), chemical composition (XRF), morphological analysis using FTIR spectroscopic and SEM-EDX analysis. Laser particle analyzer (i.e., the same equipment used in other studies such as Malvern Mastersizer 2000 and Malvern Instruments, Malvern, UK) was used in conjunction with a dispersal device for analyzing particle size distributions of the magnetic particle samples. To measure the magnetic and nonmagnetic fractions, samples underwent X-ray diffraction (XRD) with a D8-Advance Bruker with radiation of  $\text{Cu-K}\alpha$  ( $\lambda = 1.5406\ \text{nm}$ ) generated at 40 kV and 40 mA. The data were recorded in the Bragg angle ( $2\theta$ ) with a range of  $3\text{--}70^\circ$  and a scanning speed of  $2^\circ\ \text{min}^{-1}$ . To define minerals, Evaluation software 10.0 was employed with a database (PDF-2 2004) provided by International Centre for Diffraction Data.

Davies tube apparatus was used for magnetic separation. To obtain carbon-depleted and carbon-rich fractions from the samples of fly ash fraction, column floatation was used. In this regard and to perform the tests two chemicals of methyl isobutyl carbinol (MIBC) and distilled water were consumed. The carbonaceous matter was floated over the MIBC layer and was subsequently separated after the carbon-depleted fraction subsided at the bottom. To analyze the morphology of the magnetic particles and elements present in samples, scanning electron microscope (SEM) was used in conjunction with energy dispersive X-ray spectroscopy (EDS) (Quanta 450). In this study, coal chemical composition was specified indirectly. The low-temperature ash (LTA) was determined for coal samples which were subsequently analyzed for their mineral matter elements through the use of XRF. Also, feed coal underwent a sieve analysis.

The chemical composition analysis of the feed coal shows in Table 1. Such results are the sum content of  $\text{SiO}_2$ ,  $\text{Al}_2\text{O}_3$ , and  $\text{Fe}_2\text{O}_3$  is significant ( $\sim 90\%$ ). It also shows that the ash includes fewer amounts of  $\text{CaO}$ ,  $\text{K}_2\text{O}$ ,  $\text{MgO}$  and other elements. The loss on ignition (LOI) for the samples is approximately 3 and 5.6%, respectively. However, SEM analysis indicates the presence of a considerable amount of extrinsic mineral matter.

**Table 1.** The elements concentrations (%) of magnetic fractions of UB and PL fly ashes as determined by XRF analysis.

Element (%)	The Concentration of Major Elements (%) of Magnetic Fly Ash	
	UB	PL
$\text{SiO}_2$	43.64	42.85
$\text{TiO}_2$	0.83	0.76
$\text{Al}_2\text{O}_3$	21.97	21.05
T- $\text{Fe}_2\text{O}_3$	23.54	22.79
MnO	0.26	0.22
MgO	1.89	1.96
CaO	1.85	1.53

Table 1. Cont.

Element (%)	The Concentration of Major Elements (%) of Magnetic Fly Ash	
	UB	PL
Na <sub>2</sub> O	0.03	0.05
K <sub>2</sub> O	2.47	2.71
P <sub>2</sub> O <sub>5</sub>	0.22	0.2
SO <sub>3</sub>	0.34	0.47
LOI *	3.0	5.6

Note \*: Loss on ignition

According to XRF analysis of the size-fractionated fly ash samples, the total content of Fe<sub>2</sub>O<sub>3</sub>, Al<sub>2</sub>O<sub>3</sub>, and SiO<sub>2</sub> increases as the particle size decreases. Both samples display an appreciable amount of the oxides. In general, LOI decreases as the size of the particles decreases.

### 3. Results and Discussion

In this section, the three main outputs of this study including (i) particles size distribution, (ii) mineralogical analysis and (iii) morphological analysis are provided.

#### 3.1. The particle Size Distribution

As stated earlier, we used a Laser diffraction analyzer for measuring the particle size distributions of the size-fractionated fly ashes. A summary of the results obtained from the magnetic and nonmagnetic fractions is available in Figure 1 and Table 2. It can be seen from Table 2 that, more than 85% of the fly ash particles of UB and PL samples are smaller than 90 μm. Considering the results of sieve grading tests of the feed coal, an appreciable change was shown in the particle size. For a desirable burning efficiency in Pulverised Fuel Combustors, 75 μm is determined as the maximum size of the particle for the feed coal [38]. In the present case, however, larger coal particles percentage is significant, leading to inefficient combustion. Large coal particles in feed coal indicate another implication. Once the larger coal particles underwent devolatilization and during the burning of the char, will leave a noticeable mineral matter. Such outputs were quite large, meaning that these particles have been left out of further melting and fragmentation/transformation. It can be concluded that such a sieve analysis of the feed coal gives new insight into ash formation.

Table 2. Magnetic and nonmagnetic contents in different size fractions of UB and PL fly ashes.

Size (μm)	Content (%)					
	Uong Bi (UB) Fly Ash			Pha Lai (PL) Fly Ash		
	Fly ash	Magnetic	Nonmagnetic	Fly ash	Magnetic	Nonmagnetic
>250	0.41	0.14	0.27	0.33	0.12	0.21
90–250	16.48	2.03	14.45	14.48	2.59	11.89
45–90	25.58	3.52	22.06	31.19	4.62	26.57
32–45	31.18	2.43	28.75	36.66	3.23	33.43
<32	26.24	2.11	24.13	16.93	2.51	14.42
<b>Total</b>	<b>99.89</b>	<b>10.23</b>	<b>89.66</b>	<b>99.59</b>	<b>13.07</b>	<b>86.52</b>

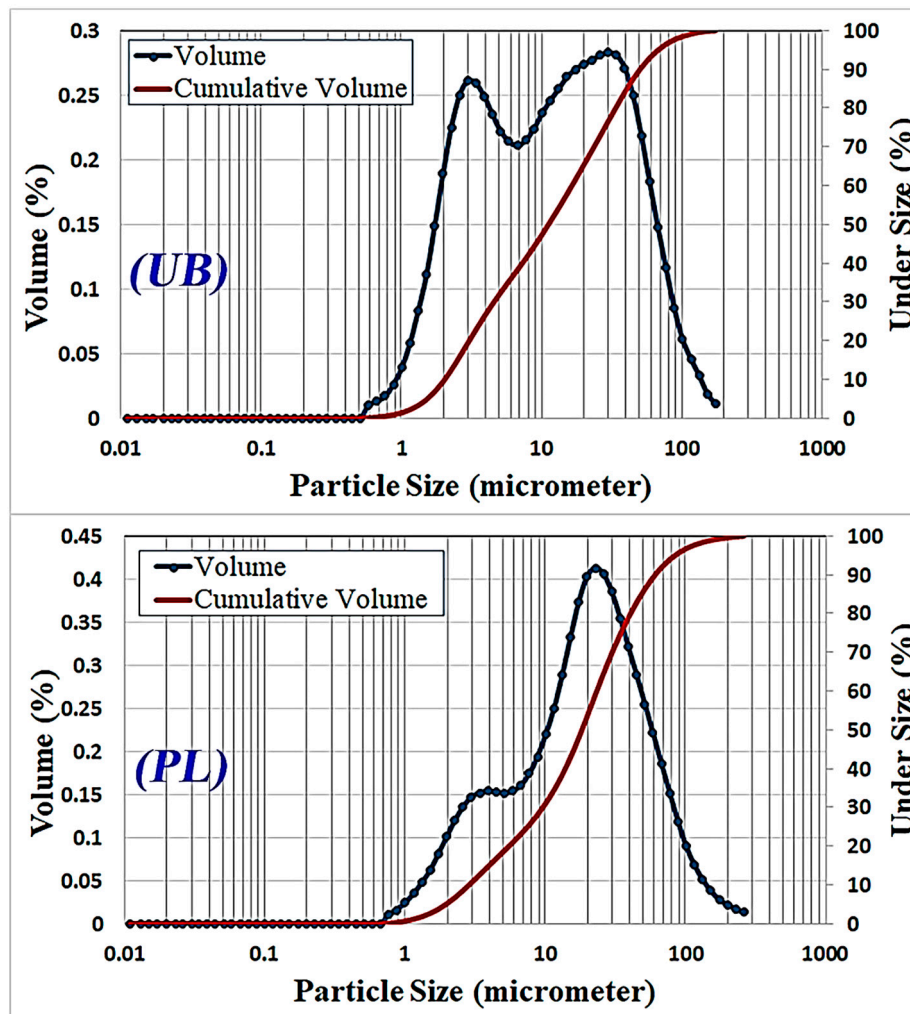


Figure 1. Particle size distribution for the magnetic fraction of UB and PL fly ashes.

According to weight percentage distribution, no certain correlation exists between the weight percentage and the size of the particles. An earlier communication has reported an exact analysis for the size of the particle of diverse size fractions such as the magnetic and non-magnetic ones and their correlations with the utility and combustion [26]. Overall, the reports indicate the larger particles are less useful for partial replacement of cement in concrete. Other researchers have also investigated the effect of particle size on the chemical composition of fly ash [17,32,33]. Those elements that display the highest concentration relevancy on particle size are mainly connected with an elemental form that sublime or boils at coal combustion temperature [11,15,37,39]. It is important to note that the Si content increases as the size of the particles decreases. This trend is apparently due to the fact that the carbon content decreases as the size of the particles decreases. Hence, it is expected that these fractions will be quite rich with Si. The rise in the Fe content in tandem with a reduction in the particle size is also fairly inconspicuous. These observations help us conclude that reduced carbon content in tandem with decreased particle size is mainly compensated by silica.

The magnetization curve of samples particles illustrated in Figure 2. The superparamagnetic properties for samples obviously can be observed. The saturation magnetization obtains for PL sample is 12.1 emu/g, and for UB sample is 4.2 emu/g. Therefore, it can be concluded the magnetite concentration in the PL sample is more than UB sample.

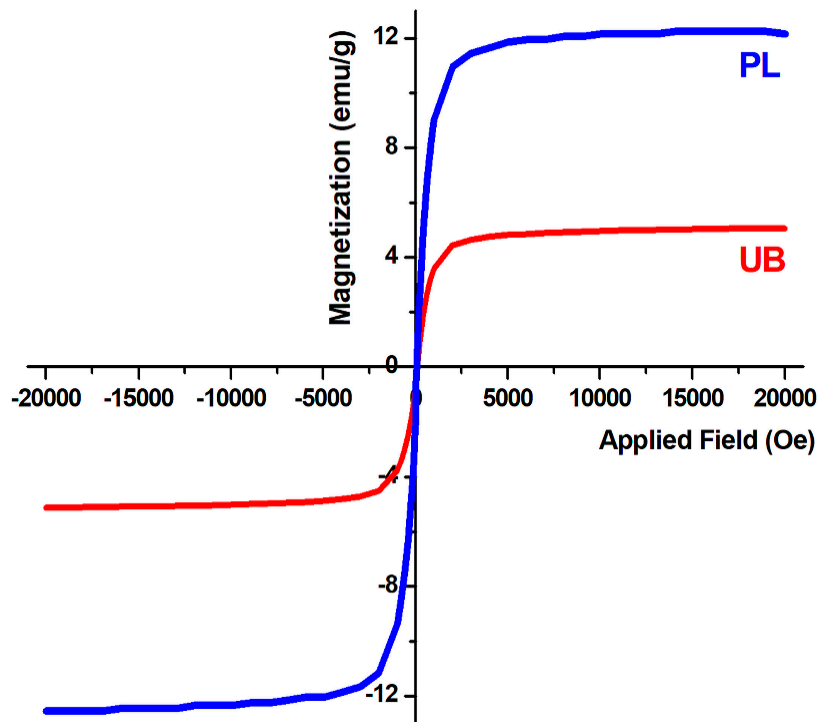
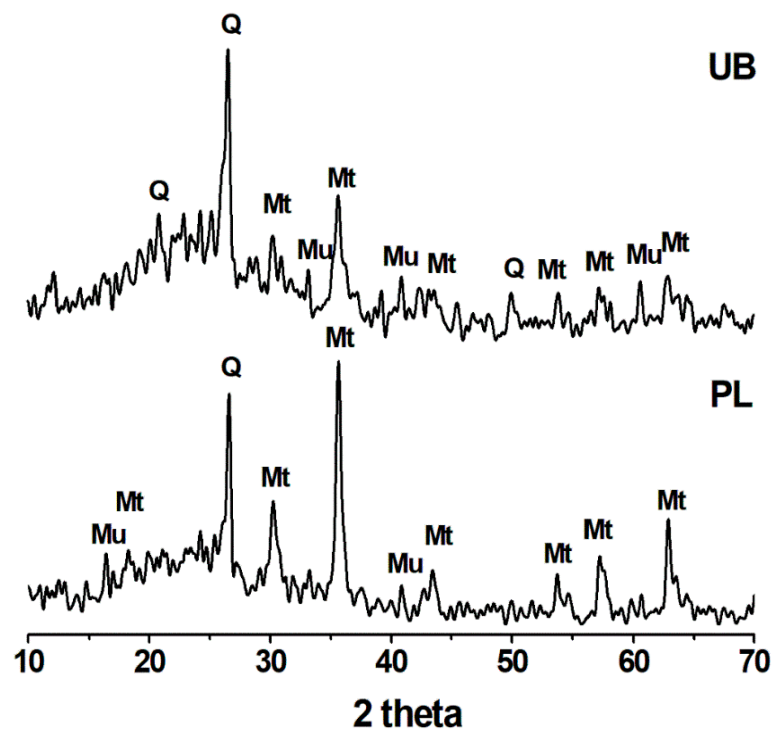


Figure 2. Magnetization vs. applied magnetic field for samples particles at 300 K.

### 3.2. Mineralogical Analysis

XRD analysis is a well-defined technique, and used in most studies (e.g., Rivera, Kaur, Hesterberg, Ward, Austin and Duckworth [25], Kaur and Goyal [18], Kunecki, Panek, Koteja and Franus [32] and Mashau, Gitari and Akinyemi [14]) to assess the fly ash's mineralogical composition. In this study, we also conducted an XRD analysis of samples. The XRD analysis was provided to acquire details on the fly ash's mineralogical composition (Figure 3). According to this analysis, the UB sample is really rich in quartz although other mineral phases like magnetite as well as mullite exist. In contrast, the PL sample is quite rich in Magnetite. Often, the non-magnetic components contain quartz and mullite as the substantial mineralogical phases. The peaks related to quartz are very intense in whole non-magnetic fractions. There is no likelihood for quantitative correlation between the particle size and the quartz content as XRD analysis is only related to qualitative approximation. However, it generally appears that the more quartz content, the lower the particle size. It is owing to refractory mullite ( $\theta = 16.4$ ). As the magnetic components indicate in this figure, magnetite and hematite produce high-intensity peaks. The point that each component contains magnetite is confirmed by good results obtained from the X-ray diffractogram tests showing an authentic sample of magnetite. These observations can be used to initiate a promising technique for the assessment of the finer magnetic fractions, that is normally essential in the preparation of coal.

Trace element analysis using ICP-MS analysis is given in Table 3. The results reveal the presence of Cr, Mn, Mg, Co, Zn, Ni, Cu, Cd, Mo, and Pb in the fly ash samples even having different concentrations (e.g., elements mentioned) in samples. Considering all the present trace elements, it is demonstrated that Pb, Mn, Cr, Cu, Zn, and Co are present with considerably higher proportions. As particle size decreases, the concentration reduction in case of Co, Mn, and Mg all of which was displaying limited to moderate concentration impact with a decrease in particle size. Cu, Cr, and Pb are adversely proportional to the size of the particle. Other elements show no significant variation in concentration with a particle size decreases.



**Figure 3.** results of XRD Analysis of the UB and PL samples. Mu: Mullite; Mt: Magnetite; Q: Quartz.

**Table 3.** Trace elements concentrations (ppm) in magnetic fractions of UB and PL fly ashes as determined ICP-MS analysis.

Element (%)	The Concentration of Trace Elements (ppm) of Magnetic Fly Ash	
	UB	PL
Co	26.13	34.27
Ni	-	-
Cu	42.92	39.38
Zn	15.51	-
Mo	1.24	1.15
Cd	-	0.23
Pb	27.22	21.73
Mn	739.38	1237.46
Mg	700.94	754.2
Cr	148.75	132.18

### 3.3. Morphological Analysis

Some interesting insights regarding the morphology of nonmagnetic and magnetic particles of Uong Bi (UB) and Pha Lai (PL) fly ash sample are revealed by Scanning electron microscopic study (SEM) (Figure 4a,b). According to Figure 4a,b, the non-magnetic and magnetic elements were found to be distinctly different. Although according to the literature, the non-magnetic components are commonly irregular in both size and shape while magnetic components generally tend to be spheroidal. However, observations of fly ash from thermal power plant showed that both magnetic and non-magnetic grains have almost spherical forms of various sizes, From the SEM results it can be concluded that particles have either a smooth or corrugated surface.

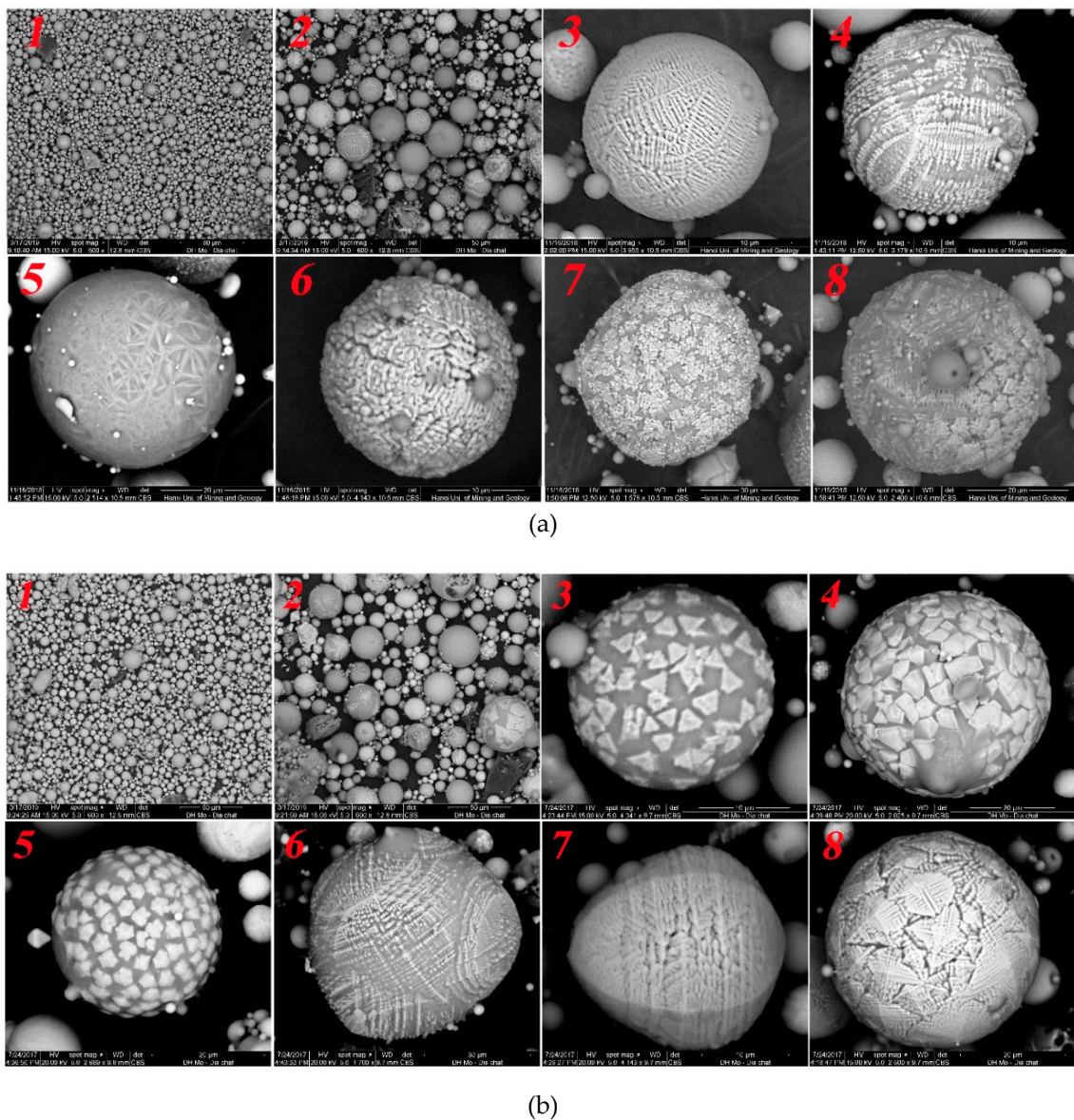
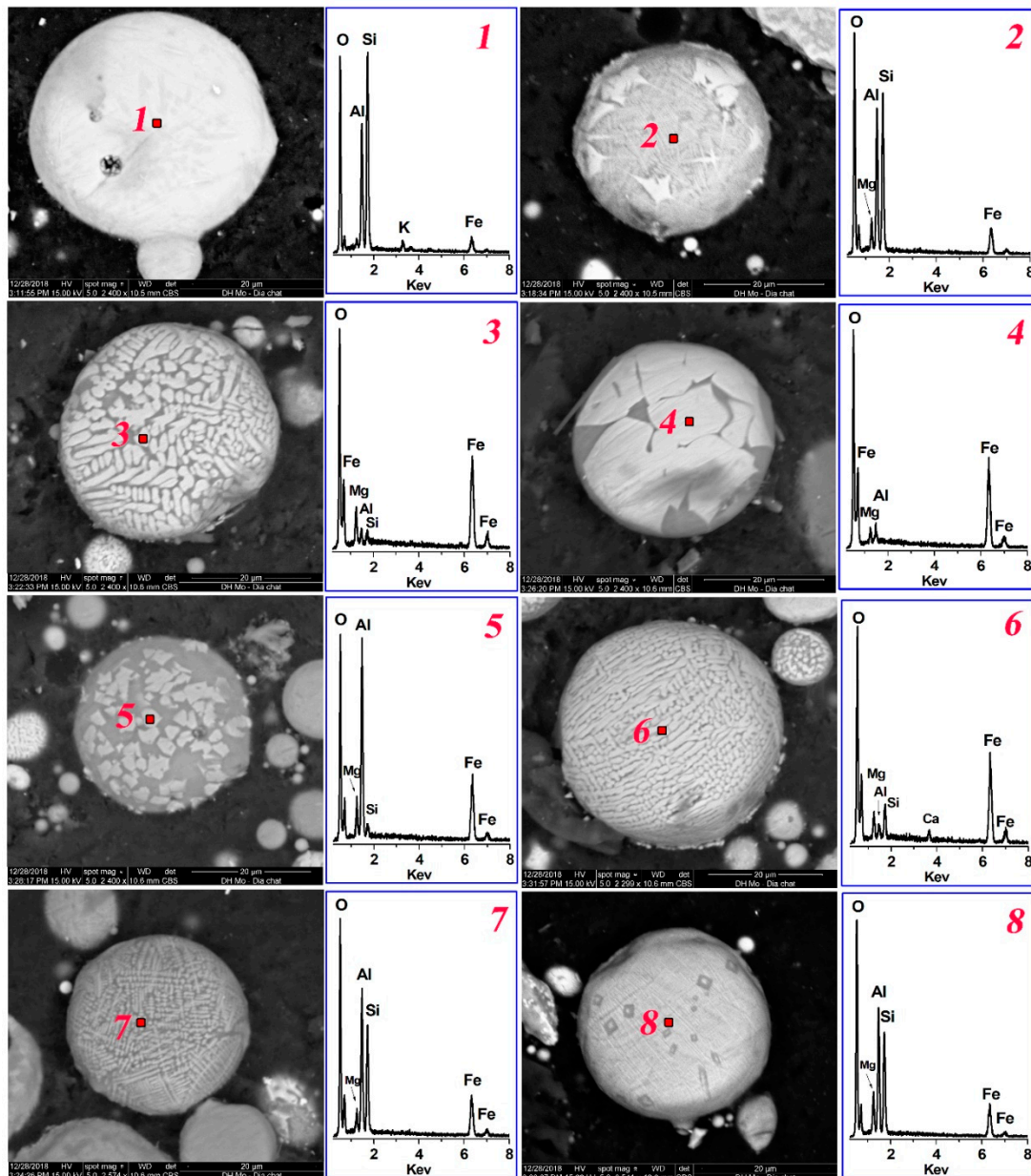


**Figure 4.** (a) Morphotypes of nonmagnetic (1) and magnetic particles (2–8) of Uong Bi (UB) fly ash; (b) Morphotypes of nonmagnetic (1) and magnetic particles (2–8) of Pha Lai (PL) fly ash.

The SEM-EDS results, shown in Figure 5a,b, indicate that the UB and PL samples contain variable amounts of Fe. The EDX analyses of magnetic fly ash indicate that the grains are mostly iron oxides although these oxides of metals were regularly present in incrustations, and some empty form. Moreover, EDX analyses reveal that the main elements are Fe and Si with Mg, Al, and K as minor elements. Although aluminum is primarily associated with silicon. Moreover, based on SEM and EDX analyses, the magnetic grains from the UB and PL samples were derived from different sources regarding the fossil fuel combustions or furnaces conditions. In fact, formation of such particles may be described in a plausible mechanism: (a) prior to fusion and melting, the mineral matters observed in coal (both extrinsic and intrinsic) undergo some transformations, (b) next, the melted matters condense and form smaller spheroidal particles, and (c) iron oxide ( $\text{Fe}^{+2}$ ,  $\text{Fe}^{+3}$ )/elemental Fe (obtained from iron carbonate in fly ash) deposit on the surfaces of these spheroidal particles.

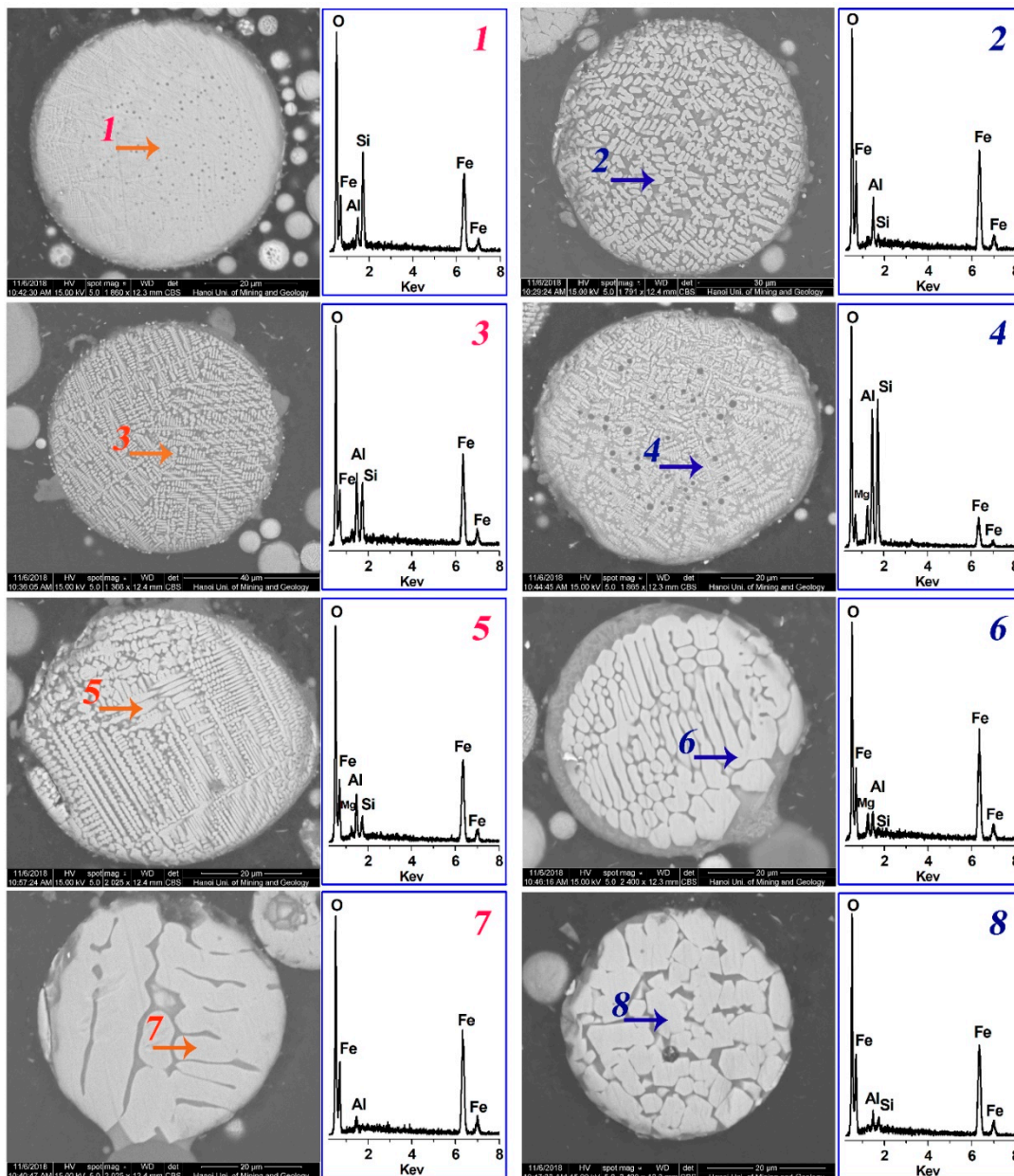
Sokol studied the condensation phenomena of iron oxides/elemental iron on the surface of the alumino-siliceous particles [40]. Other studies have also highlighted such interesting conclusions regarding the crystallite deposition on the surface of the magnetic components (e.g., Shoumkova [36], and Bourliva, et al. [41]). Accordingly, crystal deposition can take place in diverse forms and

shapes. Some magnetic particles, particularly those are related to finer fractions, are cauterized by perfect spheroidal shapes with well-classified crystallites on the surfaces. Such particles are morphologically classified in other studies as Ferrospheres (e.g., Zhang, et al. [42], Anshits, et al. [43], Anshits, et al. [44], Anshits, Fedorchak, Zhizhaev, Sharonova and Anshits [43]). The morphologies of the non-magnetic components and magnetic components of fly ash are completely different. The non-magnetic components usually have a high carbon content.



(a)

Figure 5. Cont.



(b)

**Figure 5.** (a) SEM-EDS results of Uong Bi (UB) magnetic fly ash. (b) SEM-EDS results of Pha Lai (PL) magnetic fly ash.

#### 4. Conclusions

Fly ashes are sources of many characteristic mineralogical and morphological forms of technogenic magnetic particles. The difference in the magnetic behavior of these particles refers to their mineralogical composition and crystalline structure morphology. In this research, we investigated fly ash from thermal power plants in the northern part, Vietnam. Both samples were analyzed for mineralogy by XRD analysis and SEM-EDS. The SEM imaging of PL fly ash sample shows a majority of spherical particles, which is also seen in the magnetic extracts. Investigating the morphological characteristics and the composition of fly ash give useful information on the combustion processes residual especially in the field of materials. As the main output of this study, we conclude that magnetic fractions are mainly composed of magnetite hematite and, to a lower rate, quartz, and mullite. However, after performing

the chemical analyses, it is found that the non-magnetic components consist of quartz and mullite as their primary mineral phases.

**Author Contributions:** Data collection and experimental works: D.-H.V., Q.-T.L., D.-A.N., N.-H.D.; Writing, discussion, analysis: B.K., H.-B.B., X.-N.B., H.N.

**Funding:** This work was funded by National Foundation for Science and Technology Development (NAFOSTED) in Viet Nam under grant number 105.08-2014.10.

**Acknowledgments:** The authors would like to thank the Vietnam National Foundation for Science and Technology Development (NAFOSTED) for the support under grant number 105.08-2014.10.

**Conflicts of Interest:** The authors declare no conflict of interest.

## References

1. Xu, P.; Zhao, Q.; Qiu, W.; Xue, Y.; Li, N. Microstructure and Strength of Alkali-Activated Bricks Containing Municipal Solid Waste Incineration (MSWI) Fly Ash Developed as Construction Materials. *Sustainability* **2019**, *11*, 1283. [[CrossRef](#)]
2. Gupta, N.; Gedam, V.V.; Moghe, C.; Labhassetwar, P. Investigation of characteristics and leaching behavior of coal fly ash, coal fly ash bricks and clay bricks. *Environ. Technol. Innov.* **2017**, *7*, 152–159.
3. Carlson, C.L.; Adriano, D.C. Environmental impacts of coal combustion residues. *J. Environ. Qual.* **1993**, *22*, 227–247. [[CrossRef](#)]
4. Kalaw, M.; Culaba, A.; Hinode, H.; Kurniawan, W.; Gallardo, S.; Promentilla, M. Optimizing and characterizing geopolymers from ternary blend of Philippine coal fly ash, coal bottom ash and rice hull ash. *Materials* **2016**, *9*, 580. [[CrossRef](#)] [[PubMed](#)]
5. Yao, Z.T.; Ji, X.S.; Sarker, P.K.; Tang, J.H.; Ge, L.; Xia, M.S.; Xi, Y.Q. A comprehensive review on the applications of coal fly ash. *Earth-Sci. Rev.* **2015**, *141*, 105–121. [[CrossRef](#)]
6. Hanum, F.; Desfitri, E.; Hayakawa, Y.; Kambara, S. Preliminary Study on Additives for Controlling As, Se, B, and F Leaching from Coal Fly Ash. *Minerals* **2018**, *8*, 493. [[CrossRef](#)]
7. Tomeczek, J.; Palugniok, H. Kinetics of mineral matter transformation during coal combustion. *Fuel* **2002**, *81*, 1251–1258. [[CrossRef](#)]
8. Grau, F.; Choo, H.; Hu, J.; Jung, J. Engineering behavior and characteristics of wood ash and sugarcane bagasse ash. *Materials* **2015**, *8*, 6962–6977. [[CrossRef](#)]
9. Li, X.Y.; Ma, X.W.; Zhang, S.J.; Zheng, E.Z. Mechanical Properties and Microstructure of Class C Fly Ash-Based Geopolymer Paste and Mortar. *Materials* **2013**, *6*, 1485–1495. [[CrossRef](#)]
10. Tigue, A.A.S.; Malenab, R.A.J.; Dungca, J.R.; Yu, D.E.C.; Promentilla, M.A.B. Chemical Stability and Leaching Behavior of One-Part Geopolymer from Soil and Coal Fly Ash Mixtures. *Minerals* **2018**, *8*. [[CrossRef](#)]
11. Du Plessis, P.W.; Ojumu, T.V.; Fatoba, O.O.; Akinyeye, R.O.; Petrik, L.F. Distributional Fate of Elements during the Synthesis of Zeolites from South African Coal Fly Ash. *Materials* **2014**, *7*, 3305–3318. [[CrossRef](#)]
12. Du Plessis, P.W.; Ojumu, T.V.; Petrik, L.F. Waste Minimization Protocols for the Process of Synthesizing Zeolites from South African Coal Fly Ash. *Materials* **2013**, *6*, 1688–1703. [[CrossRef](#)] [[PubMed](#)]
13. Darsanasiri, A.; Matalakah, F.; Ramli, S.; Al-Jalode, K.; Balachandra, A.; Soroushian, P. Ternary alkali aluminosilicate cement based on rice husk ash, slag and coal fly ash. *J. Build. Eng.* **2018**, *19*, 36–41. [[CrossRef](#)]
14. Mashau, A.S.; Gitari, M.W.; Akinyemi, S.A. Evaluation of the Bioavailability and Translocation of Selected Heavy Metals by Brassica juncea and Spinacea oleracea L for a South African Power Utility Coal Fly Ash. *Int. J. Environ. Res. Public Health* **2018**, *15*. [[CrossRef](#)] [[PubMed](#)]
15. Asl, S.M.H.; Javadian, H.; Khavarpour, M.; Belviso, C.; Taghavi, M.; Maghsudi, M. Porous adsorbents derived from coal fly ash as cost-effective and environmentally-friendly sources of aluminosilicate for sequestration of aqueous and gaseous pollutants: A review. *J. Clean. Prod.* **2019**, *208*, 1131–1147.
16. Sun, P.; Sun, D.S.; Wang, A.G.; Ge, W.B.; Liu, X.L. Preparation and Properties of Sintered Brick Based on Coal Gangue and Fly Ash. *Asian J. Chem.* **2014**, *26*, 1517–1520. [[CrossRef](#)]
17. Van der Merwe, E.M.; Prinsloo, L.C.; Mathebula, C.L.; Swart, H.C.; Coetsee, E.; Doucet, F.J. Surface and bulk characterization of an ultrafine South African coal fly ash with reference to polymer applications. *Appl. Surf. Sci.* **2014**, *317*, 73–83. [[CrossRef](#)]

18. Kaur, R.; Goyal, D. Mineralogical comparison of coal fly ash with soil for use in agriculture. *J. Mater. Cycles Waste Manag.* **2016**, *18*, 186–200. [[CrossRef](#)]
19. Kostova, I. Geochemical Characterization and Mercury Content of Feed Coals And Fly Ashes From Russe Thermoelectric Power Plant, Bulgaria. *Comptes Rendus De L Academie Bulgare Des Sciences* **2017**, *70*, 829–838.
20. Wei, C.D.; Cheng, S.; Zhu, F.J.; Tan, X.L.; Li, W.Q.; Zhang, P.P.; Miao, S.D. Digesting high-aluminum coal fly ash with concentrated sulfuric acid at high temperatures. *Hydrometallurgy* **2018**, *180*, 41–48. [[CrossRef](#)]
21. Wu, D.Y.; Sul, Y.; Chen, X.C.; He, S.B.; Wang, X.; Kong, H. Changes of mineralogical-chemical composition, cation exchange capacity, and phosphate immobilization capacity during the hydrothermal conversion process of coal fly ash into zeolite. *Fuel* **2008**, *87*, 2194–2200. [[CrossRef](#)]
22. Zhao, Y.C.; Zhang, J.Y.; Tian, C.; Li, H.L.; Shao, X.Y.; Zheng, C.G. Mineralogy and Chemical Composition of High-Calcium Fly Ashes and Density Fractions from a Coal-Fired Power Plant in China. *Energy Fuels* **2010**, *24*, 834–843.
23. Akinyemi, S.A.; Akinlua, A.; Gitari, W.M.; Petrik, L.F. Mineralogy and Mobility Patterns of Chemical Species in Weathered Coal Fly Ash. *Energy Sources Part A Recovery Util. Environ. Eff.* **2011**, *33*, 768–784. [[CrossRef](#)]
24. Cvetkovic, Z.; Logar, M.; Rosic, A.; Ciric, A. Mineral composition of the airborne particles in the coal dust and fly ash of the Kolubara basin (Serbia). *Periodico Di Mineralogia* **2012**, *81*, 205–223.
25. Rivera, N.; Kaur, N.; Hesterberg, D.; Ward, C.R.; Austin, R.E.; Duckworth, O.W. Chemical Composition, Speciation, and Elemental Associations in Coal Fly Ash Samples Related to the Kingston Ash Spill. *Energy Fuels* **2015**, *29*, 954–967.
26. Koukouzas, N.; Ward, C.R.; Papanikolaou, D.; Li, Z.S.; Ketikidis, C. Quantitative evaluation of minerals in fly ashes of biomass, coal and biomass-coal mixture derived from circulating fluidised bed combustion technology. *J. Hazard. Mater.* **2009**, *169*, 100–107. [[CrossRef](#)] [[PubMed](#)]
27. Koukouzas, N.; Ketikidis, C.; Itskos, G. Heavy metal characterization of CFB-derived coal fly ash. *Fuel Process. Technol.* **2011**, *92*, 441–446. [[CrossRef](#)]
28. Telesca, A.; Marroccoli, M.; Calabrese, D.; Valenti, G.L.; Montagnaro, F. Flue gas desulfurization gypsum and coal fly ash as basic components of prefabricated building materials. *Waste Manag.* **2013**, *33*, 628–633. [[CrossRef](#)] [[PubMed](#)]
29. Koukouzas, N.K.; Zeng, R.S.; Perdikatsis, V.; Xu, W.D.; Kakaras, E.K. Mineralogy and geochemistry of Greek and Chinese coal fly ash. *Fuel* **2006**, *85*, 2301–2309. [[CrossRef](#)]
30. Koukouzas, N.; Hamalainen, J.; Papanikolaou, D.; Tourunen, A.; Jantti, T. Mineralogical and elemental composition of fly ash from pilot scale fluidised bed combustion of lignite, bituminous coal, wood chips and their blends. *Fuel* **2007**, *86*, 2186–2193. [[CrossRef](#)]
31. Shoumkova, A.; Stoyanova, V. Zeolites formation by hydrothermal alkali activation of coal fly ash from thermal power station “Maritsa 3”, Bulgaria. *Fuel* **2013**, *103*, 533–541. [[CrossRef](#)]
32. Kunecki, P.; Panek, R.; Koteja, A.; Franus, W. Influence of the reaction time on the crystal structure of Na-P1 zeolite obtained from coal fly ash microspheres. *Microporous Mesoporous Mater.* **2018**, *266*, 102–108. [[CrossRef](#)]
33. He, P.; Jiang, X.M.; Wu, J.; Pan, W.G.; Ren, J.X. Characterization Of Fly Ash From Coal-Fired Power Plant And Their Properties Of Mercury Retention. *Surf. Rev. Lett.* **2015**, *22*. [[CrossRef](#)]
34. Izidoro, J.D.; Fungaro, D.A.; dos Santos, F.S.; Wang, S.B. Characteristics of Brazilian coal fly ashes and their synthesized zeolites. *Fuel Process. Technol.* **2012**, *97*, 38–44. [[CrossRef](#)]
35. Moreno, N.; Querol, X.; Andres, J.M.; Stanton, K.; Towler, M.; Nugteren, H.; Janssen-Jurkovicova, M.; Jones, R. Physico-chemical characteristics of European pulverized coal combustion fly ashes. *Fuel* **2005**, *84*, 1351–1363. [[CrossRef](#)]
36. Shoumkova, A.S. Magnetic separation of coal fly ash from Bulgarian power plants. *Waste Manag. Res.* **2011**, *29*, 1078–1089.
37. Sow, M.; Hot, J.; Tribut, C.; Cyr, M. Characterization of Spreader Stoker Coal Fly Ashes (SSCFA) for their use in cement-based applications. *Fuel* **2015**, *162*, 224–233. [[CrossRef](#)]
38. Sarkar, A.; Rano, R.; Udaybhanu, G.; Basu, A. A comprehensive characterisation of fly ash from a thermal power plant in Eastern India. *Fuel Process. Technol.* **2006**, *87*, 259–277. [[CrossRef](#)]
39. Dos Santos, R.P.; Martins, J.; Gadelha, C.; Cavada, B.; Albertini, A.V.; Arruda, F.; Vasconcelos, M.; Teixeira, E.; Alves, F.; Lima, J.; Freire, V. Coal Fly Ash Ceramics: Preparation, Characterization, and Use in the Hydrolysis of Sucrose. *Sci. World J.* **2014**. [[CrossRef](#)]

40. Sokol, E.; Kalugin, V.; Nigmatulina, E.; Volkova, N.; Frenkel, A.; Maksimova, N. Ferrospheres from fly ashes of Chelyabinsk coals: Chemical composition, morphology and formation conditions. *Fuel* **2002**, *81*, 867–876. [[CrossRef](#)]
41. Bourliva, A.; Papadopoulou, L.; Aidona, E.; Simeonidis, K.; Vourlias, G.; Devlin, E.; Sanakis, Y. Enrichment and oral bioaccessibility of selected trace elements in fly ash-derived magnetic components. *Environ. Sci. Pollut. Res.* **2017**, *24*, 2337–2349. [[CrossRef](#)] [[PubMed](#)]
42. Zhang, K.H.; Zhang, D.X.; Zhang, K.; Cao, Y. Capture of Gas-Phase Arsenic by Ferrospheres Separated from Fly Ashes. *Energy Fuels* **2016**, *30*, 8746–8752.
43. Anshits, N.N.; Fedorchak, M.A.; Zhizhaev, A.M.; Sharonova, O.M.; Anshits, A.G. Composition and Structure of Block-Type Ferrospheres Isolated from Calcium-Rich Power Plant Ash. *Inorg. Mater.* **2018**, *54*, 187–194. [[CrossRef](#)]
44. Anshits, N.N.; Fedorchak, M.A.; Zhizhaev, A.M.; Anshits, A.G. Structure-Composition Relationship of Skeletal and Dendritic Ferrospheres Isolated from Calcium-Rich Power Plant Ash. *Inorg. Mater.* **2018**, *54*, 253–260. [[CrossRef](#)]



© 2019 by the authors. Licensee MDPI, Basel, Switzerland. This article is an open access article distributed under the terms and conditions of the Creative Commons Attribution (CC BY) license (<http://creativecommons.org/licenses/by/4.0/>).